Viscous Effects on Granular Mixtures in a Rotating Drum

Miguel Angel Cabrera[1], Devis Gollin[2], Roland Kaitna[3], and Wei Wu[1]

[1] Institut für Geotechnik, Universität für Bodenkultur, Vienna, Austria
[2] Department TESAFLand, Environment, Agriculture and Forestry, University of Padova, Viale dell'Università 16, 35020 Legnaro, PD, Italy
[3] Institut für Alpine Naturgefahren, Universität für Bodenkultur, Vienna, Austria
miguel.cabrera@boku.ac.at

Abstract. In debris flow research, fine particles are considered to be part of the fluid phase of the flow. Nonetheless the particle-size threshold of this phase is not generally clear and could be dependent on the motion-characteristics of the flow itself. In the present study, rotating drum experiments are employed to investigate the effects of kaolin and silt fractions mixed in a fluid phase over a granular mixture of fine and coarse sand. Eight soil mixtures were prepared and tested at variable rotational velocities and water content. The mixtures are subjected to a constant shear that shifts the tested material and due to the action of gravitational forces a recirculating flow is produced inside the rotating drum. Our experiments found evidence of a solid concentration limit value where a shear-dependent behaviour is developed in the mixtures.

Keywords: Granular flows, Rotating drum, kaolin, loess.

1 Introduction

In mountain areas after intense periods of rain or ice melting seasons, the saturation of slopes leads to mass flows involving large volumes of soil, water, and vegetation. These mass flows are often referenced as debris flows, mud flows, debris flood, debris avalanche, and earth flows [9]. A better understanding of those flows will lead to an improvement in prevention systems, saving lives, property, and protecting productive land.

In the case of debris flows, sand, gravel, and larger boulders compose most of the mass of the debris, whereas silt and clay-sized grains commonly constitute less than 10% of the mass [4], [11]. On the other hand, mud flows have a higher fines fraction and fewer boulders [9], [22].

The particle size distribution (PSD) of the mass flow directly affects the evolution of the stresses during motion. In the case of coarse particles, internal forces arise from short-term collisions or long-term frictional forces between the grains. The presence of fine particles suspended in the fluid might increase viscosity and

© Springer International Publishing Switzerland 2015

W. Wu (ed.), *Recent Advances in Modeling Landslides and Debris Flows*,
Springer Series in Geomechanics and Geoengineering, DOI: 10.1007/978-3-319-11053-0_6

bulk density of the fluid [5]. Therefore, homogeneous mixtures of water and fine sediment can be described with a simple shear-strain relation [3].

The current work aims, through experimental modelling, to provide evidence of the interaction of a highly viscous fluid in a granular flow. Rotating drum experiments with debris flows (also known as vertical rotating flume experiments [15]) were initially developed by [2] and [8].

In order to clarify the interaction of coarse and fine particles at different water contents a parametric study in the rotating drum was developed. Coarse and fine sand were employed to represent the solid phase of the granular flow, and loess and kaolin (kaolinite clay) were mixed with water to produce a fluid with an increased viscosity. Drum tests were conducted in two sets. The first set of tests focused on the rheological behaviour of the source granular materials as reference tests, while the second set tested the rheological behaviour of the interaction of the granular materials with the addition of kaolin and loess at different water contents.

On dry conditions, granular flows (sand mixtures) are expected to be less affected by the variation of the rotational velocity of the drum. When enduring frictional contacts prevail, resistance is expected to be defined by the grains contact parameters, which show non- or low-shear dependent behaviour following a Coulomb model [11] [14]. With the addition of water and increased viscous water-mixtures it is intended to weaken the particle interactions and obtain a shear-dependent response from the fluid phase. The shear-dependent response of the flow is expected to present a power law distribution as in a non-Newtonian fluid [28].

In this paper section 2 presents the description of the rotating drum, its instrumentation, the characteristics of the soil mixtures, and the test routine. Section 3 discusses the governing equations of granular flows induced in the rotating drum and describes the assumptions adopted in the data analysis. Section 4 presents the results obtained from the measurement system of the drum, discusses the characteristics of the flows tested, and analyses the characteristics of granular flows saturated with a viscous fluid. Section 5 discusses the obtained results, and provides some recommendations for future work.

2 Methods

The rotating drum is composed of a rotating cylindrical channel section connected to an engine that imposes a controlled rotational velocity (see Fig. 1). The material inside the drum is dragged at a constant velocity by the roughened surface and lateral walls, until an avalanche is released at the apex of the flow with an equivalent velocity. This recirculating process is self balancing giving the characteristics of a steady-state flow. The main advantage of employing a rotating drum is the opportunity to establish stationary conditions over an extended period of time [17].

2.1 Apparatus and Instrumentation

The experiments were performed in a rotating drum with an inner diameter of 2.46 m and channel width of 0.45 m at the University of Natural Resources and Life Sciences (BOKU), Vienna, Austria. The rotating drum has a rectangular inner section (Fig. 1). The side-walls are composed at one side of stainless steel and at the opposite side of acrylic glass [17]. The bed of the channel is roughened using a rubber surface with protrusions in a zigzag pattern of approximately 3 mm in height and 5 mm in separation.

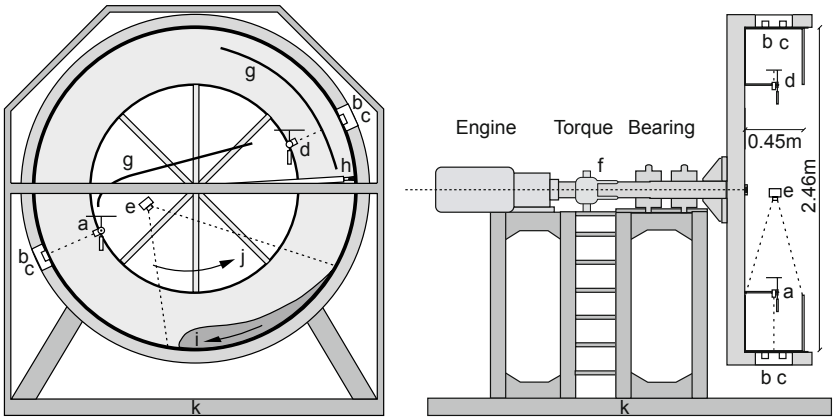

Fig. 1. Rotating drum at BOKU. a) Height point-laser, b) Normal load cell, c) Shear load cell d) Height ultrasonic sensor, e) High-speed camera, f) Sliced ring, g) Inner-roof (drop protection), h) Broom (controls mass up-flow), i) Material flow direction, j) Drum rotating direction, k) Steel frame. Adapted from [17] and [26].

The rotational velocity of the drum is measured with a sliced-ring fixed together with the thrust bearing. A static photo-electric sensor records an impulse at every degree of rotation, thus the angular position of each sensor installed within the drum can be traced. The rotational velocity of the drum is measured at the sliced ring in revolutions per minute (rpm).

Two load cells (HBM PW2GC3) are employed to measure normal forces at the base of the channel section. The load cells are installed at two different locations along the circumference displaced 180° (Fig. 1). Each load cell is connected to a plate, 60 mm in diameter, covered by the same roughened rubber of the drum's bed. This arrangement gives two independent normal force measurements at the third of the drum channel base. In order to prevent leaking and clogging of material the edges of the plates were sealed with a thin silicone layer. Due to the rotation, the recorded signal has a sinusoidal shape caused by the self weight of the assemblage. This sinusoidal effect was removed in the post-processing with a digital signal filtering procedure [26].

Above the load cells, the flow depth was measured by an ultra-sonic sensor (Pepperl und Fuchs UC500-30GM) and a point-laser sensor (Baumer OADM 20) at the same location as the load cells, installed on the central position of the channel cross-section. Near the center of rotation a high-speed camera (Casio EX-ZR15) recorded the full extension of the granular flow at a rate of 232 fps with a frame size of 512×384 pixels (Fig. 1).

The sliced-ring, load cells, and ultrasonic and laser sensors were recorded using a data acquisition system at a sampling frequency of 1200 Hz.

2.2 Soil Mixtures

Mixtures of coarse and fine sand were selected to represent the reference framework, in which the effect of fluid properties are investigated. First with the addition of water, then with the addition of loess and kaolin (kaolinite clay) mixed with water, to produce a fluid with an increased viscosity. Fig. 2 presents the particle size distributions (PSD) of the source materials and mixture compositions.

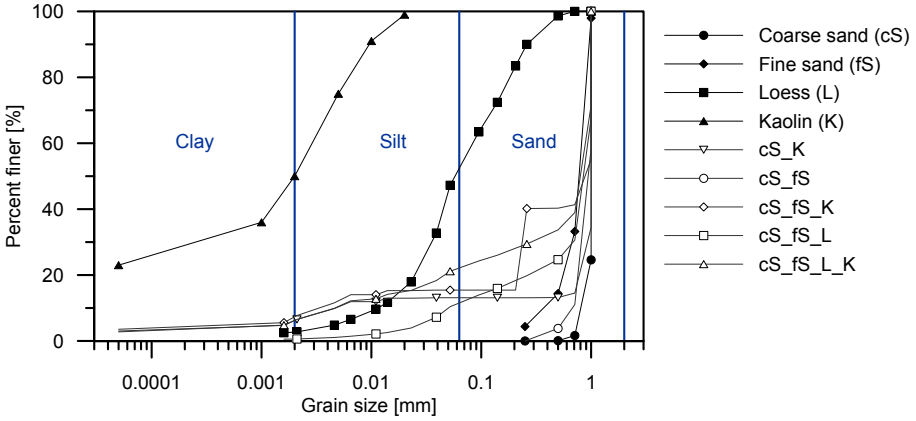

Fig. 2. Particle size distribution (PSD) of the materials tested. Note that the filled dots present the PSD of the source materials, and the empty dots denote the resulting PSD of the mixtures. For more details about the mixtures see table 1.

The sand is a standard naturally rounded siliceous sand (normsand DIN-1164) and a fine high-purity quartz sand. The material is selected because its uniform particle shape and poorly graded PSD (Fig. 2). The mean particle size of the sand samples is 1 mm and 0.71 mm respectively.

Loess is a silty sediment of high porosity, deposited by aeolian action, which can be "draped" across the landscape [13] and known for its high content of silt-size particles [27]. The silt fraction was obtained from a loess deposit in Austria. To define both, the particle size distribution and the silt portion of the loess, a

mechanical gradation and hydrometer method was performed. The results show that 2.6% was composed of clay, 50.6% of slit, and 46.9% of sand (Fig. 2). Note that the silt fraction was not sieved separately from the sample, herein the three fractions employed in tests are presented together in the PSD L on Fig. 2.

Kaolinite clay (Kamig-E1) with mean particle size 2 μm (PSD given by the producer) is chosen because of its low reactivity, particularly compared to other common clays (e.g. bentonite) [21], and for the known viscous properties when it is mixed with water [1], [6], [22]. The rheology of the kaolin-water and loess-water dispersions is quantified using a simple co-axial cylinder rheometer (Bohlin Visco 88). In order to measure the viscosity of the silt fraction, the loess sample material is sieved in order to avoid material jamming at the inner cylinder of the rheometer. The solid concentration Cv of the fine-soil-water mixtures, defined as the ratio of the solid volume V_s (fines and coarse particles) over the total volume V_t of the mixture ($Cv = V_s/V_t$), ranges between 0.50 to 0.70.

Fig. 3 shows the shear flow curves for kaolin and loess. The results show a non-Newtonian shear dependent behaviour for both dispersions. In the case of kaolin and loess the viscosity increases with the solid concentration, and decays to a constant value at high shear rates. Note that for the loess dispersion at a Cv value of 0.42 irregular results are obtained at high shear stress values. This could be due to short grain "jams" caused by clogging of material during measurements at this particular Cv.

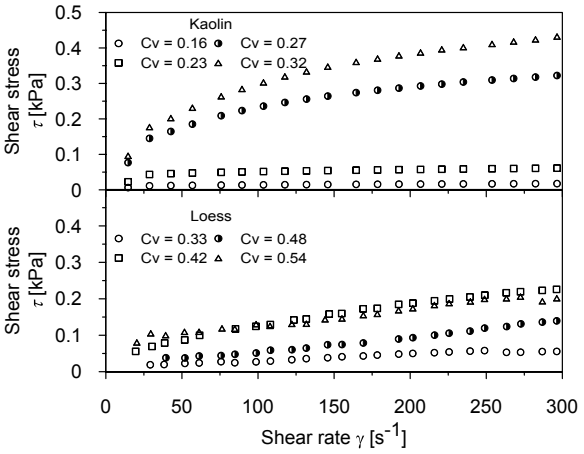

Fig. 3. Viscosity curves for kaolin and loess mixed with water at different solid concentrations (Cv)

2.3 Test Routine

Drum tests were performed in two sets with different grain size fractions (Table 1). For listing purposes the mixture names are followed by the bulk solid concentration of the mixture Cv and the rotational velocity of the test, for example

cS_fS_0.65_7 stands for the mixture of coarse sand and fine sand with a Cv value of 0.65 at 7 rpm. Note that the mixture cS_K1 has a lower content of kaoline than cS_K2 (Cv of kaolin of 0.23 and 0.27 respectively), and thus it is expected that the viscous effects of the mixture cS_K2 become stronger than cS_K1.

Table 1. Rotating drum tests. The abbreviations stands for, cS: coarse sand, fS: fine sand, L: loess, and K: kaolin.

Set	Mixture name	Mass fraction [%]	Solid Concentration Cv [-]
1	cS	100	*dry* 0.65 0.60 0.56 0.52 0.49
	cS_fS	70-30	*dry* 0.65 0.60 0.56 0.52 0.49
	L	100	- 0.53 0.50 0.47 0.45 0.43
2	cS_K1	88.5-11.5	0.71 0.66 0.61 0.57 0.53 0.50
	cS_K2	87.3-12.7	0.74 0.67 0.61 0.57 0.53 0.50
	cS_fS_K	61.9-26.5-11.5	0.71 0.66 0.61 0.57 0.53 0.50
	cS_fS_L	54.6-23.4-22.0	0.72 0.65 0.60 0.56 0.52 0.48
	cS_fS_L_K	48.0-20.6-19.4-12	0.69 0.65 0.60 0.56 0.52 0.49

Every test started with the weighing of the granular material and fluid phase according to a previous defined fraction (Table 1). The total mass of the tested material was approximately 50 kg, and the addition of water to the mixture ranged from 7 to 20 L. Mixtures with different grain size gradation were mixed in a mortar mixer to ensure an homogeneous mixture. During the mixing process, a Cv value was reached by adding a known amount of water. After the mixture become homogeneous, it was added to the rotating drum.

Once the drum was filled a couple of rotations were completed in order to check the sensors response and allow the roughened surface to be uniformly covered by the material. Rotational velocities of 3, 5, 7, and 9 rpm were applied to the mixtures (0.40, 0.65, 0.90, 1.20 ms^{-1}, respectively). The materials were tested over 7 to 10 rotations, during each set of velocities. When the rotational cycle finishes, a previously weighed amount of water is added to the mixture inside the drum (changing the solid concentration Cv of the mixture and of the fluid phase) and the rotational cycle starts again. Five to six cycles of varying the Cv per granular mixture were executed.

3 Governing Principles

Considering a continuum approach, as widely developed by [11], [10], [24], and [25] the governing laws for free surface flows are defined by the balance of mass and momentum (Eq. 1 and 2). A balance of mass considers the flowing material to be fixed to a value and avoid mass changes during flow, and the balance of momentum considers the equilibrium of acting forces during flow. In this case, the physical laws are written as a function of the mixture's density ρ, the velocity

vector $\mathbf{v}$, the stress tensor $\mathbf{T}$, and the gravitational field $\mathbf{g}$. Note that in a two phase flow the contributions of the fluid and solid constituents can be treated independently.

$$\frac{\partial \rho}{\delta t} + \nabla \cdot \rho \mathbf{v} = 0 \tag{1}$$

$$\frac{\partial v}{\partial t} + \nabla \cdot \rho v \otimes v - \nabla \cdot \mathbf{T} + \rho g = 0 \tag{2}$$

The stress tensor is the result of the interactions inside and between the different phases present in the flow. According to [12], [23] and [28] these interactions are identified as:

- short-term collisions of coarse particles,
- enduring particle friction (long-term contacts),
- deformation of the fluid phase (viscous shear),
- stresses between particles and fluid resulting from the relative motion of the fluid and solid constituents (Drag and buoyancy).
- macro turbulent mixing of the fluid phase and coarse particles (inertial velocity fluctuations),

Understanding of the interactions allows recognizing different dominant sources of flow resistance. In dry tests the collisions and frictional forces between particles will be the only interactions present in the flow. While, when a liquid is added to the flow and depending on its viscosity, the fluid interactions start becoming dominant.

Assuming an homogeneous flow and in order to simplify the motion characteristics, the torque (T) is assumed to act at the center of mass of the granular flow and defines the shear applied to the material. The angle (α) between the center of the drum and the center of mass is considered as an equivalent slope angle as presented in Fig. 4 [17], [18], [26]. In this sense, T is computed from the total weight of the granular mixture ($\rho g V$) times the horizontal distance between the center of the drum and the center of mass of the surge ($r_0 \sin \alpha$) (Eq. 3).

$$T = \rho g V r_0 \sin \alpha \tag{3}$$

Then, the mean shear stresss (τ_{mean}) is estimated considering a constant distribution of shear through the area in contact with the granular flow [16]. It is assumed an equal distribution of the bed shear stress and a lineal shear stress distribution on the side-walls (Eq. 4).

$$\tau_{mean} = \frac{T}{A_b r + A_s (r - h_{mean}/3)} \tag{4}$$

Where r is the radius of the drum, h_{mean} is the mean height of the flow and, A_b and A_s are the equivalent area of the flow at the base and cross-section of the drum, respectively.

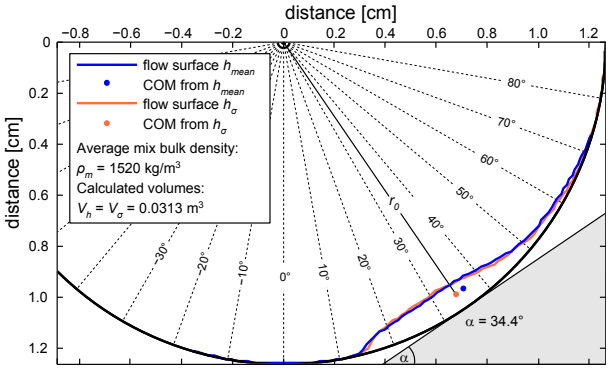

Fig. 4. Calculation of center of mass shown for the mixture cS_fS_0.52_5. Note that the height profiles obtained from the laser measurements (h_mean) are in agreement with the post processed load cell measurements (h_σ). The 0° point inside the drum is located at 6 o'clock for reference purposes.

4 Results and Analysis

The flow height and normal stress measurements are averaged every degree of rotation. Measured data are found to oscillate more frequently in the tail of the surge profile. These oscillations are considered to be generated by internal development of surges at the tail of the flow.

4.1 General Observations

Granular flows tested in the rotating drum (cS and cS_fS) show specific patterns whether the material was dry or in addition of water. At dry conditions, the pattern of velocities at the surface are affected by the lateral walls generating a middle channel with higher velocities, with a longer body and a shorter tail. Once water is added to the granular material, the effect of the lateral walls decreases and the granular flow transforms into a plug, shortening the body and elongating the tail.

For the coarse grain test (cS) the increase in water content reach a limit level where the mixture of water and soil grains remains in the same bulk flowing mass (Cv of 0.56). At low rotational velocities, the water starts to percolate to the front of the flow and separate from the sand body. Nonetheless, once the rotational velocity of the drum increases, the percolation ceases and the mixture of the two phases is achieved. Similar cases are observed at higher water contents for the mixture of coarse and fine sand (Cv of 0.52), for the mixtures with kaolin (Cv of 0.66 and 0.67), and with loess (Cv of 0.47). Full phase mixing is not evident for the mixture cS_fS_K_L. Therefore, it is possible to conclude that the percolation process (or phase separation) is associated with the porosity of the granular mixture, the viscosity of the fluid phase, and the stress state happening in the flowing mixture as presented in [19].

It is important to note that for the tests with kaolin at high volumetric concentrations ($Cv \geq 0.61$), the losses of material are significant; losing more than 25% of the material in one cycle of rotational velocities. The losses occur due to the clogging of material in the roughened bed followed by dropping and accumulation in the inner roof of the drum (Fig. 1 part f). The losses of material are recognized as one of the biggest limitations of the tests, and are not considered in the following analysis.

At high solid concentrations and high rotational velocities, the thickness of the tail becomes considerably smaller. Then, the drag forces induced by the drum's bed become stronger than the acting forces in the flow direction, generating a separation in the body of the flow. This process caused the creation of internal surges in the tail of the flow at low Cv values, and is considered as one of the reasons for the material losses at high Cv values.

Particle image velocimetry (PIV) analysis were applied on the high-speed recordings. The PIV analyses were computed with the open source code PIVlab (v.1.32). The velocity field obtained on the PIV analysis (Fig. 5.a) enables to infer the location of the front, body and tail of the granular flow. Highest velocities occur at the front mid-section (e.g., zone of 0.2 m/s in Fig. 5.b), then the distribution of the superficial velocities flattens making a transition through the body to the tail where the values are almost negligible.

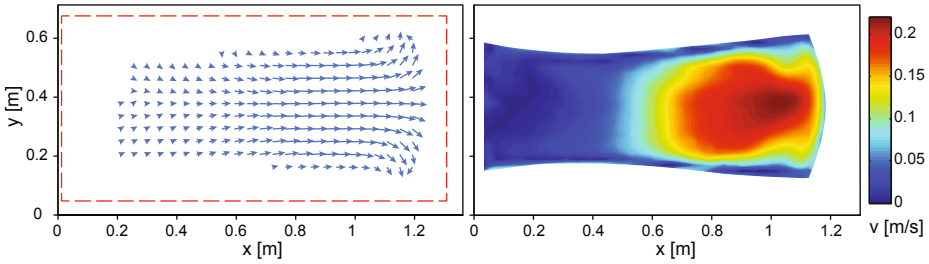

Fig. 5. Particle Image Velocimetry (PIV) of the recorded high-speed videos on the test cS_K1_0.71_3. The left image shows the average velocity field (1304 frames), and the right image shows the distribution of the velocity magnitude on surface.

The velocity field is symmetric across the mid-section of the channel for the flows with high Cv values. When the mixture becomes more fluid the symmetry-axis is displaced. In those cases the front tended to move faster in proximity to the aluminium wall, assumed to have a larger friction coefficient than the acrylic wall.

The velocity field in Fig. 5.a shows that the direction of the velocity vectors varies in space making a strongly non-uniform flow. However the magnitude and direction of the velocity at each point of analysis is usually constant in time. This indicates that the flows induced inside the rotating drum are non-uniform quasi-steady flows.

4.2 Viscous Effects on Granular Mixtures

In order to elucidate the shear-dependent behaviour Fig. 6 presents the height profiles of the mixtures at different rotational velocities for the range of Cv values between 0.67 to 0.69. The obtained results identify the starting point of the flow and the dependence on mixture composition. Granular flows (cS and cS_fS) in the presence of water started at steeper locations inside the drum, while flows with increased viscosity (with the addition of L and K) were found at lower zones. This behaviour might be due to the effect of the induced shear stress inside the drum being supported by the grains in flows with water, rather than in flows where the presence of loess and kaolin increases the density and viscosity of the fluid that surrounds the grains.

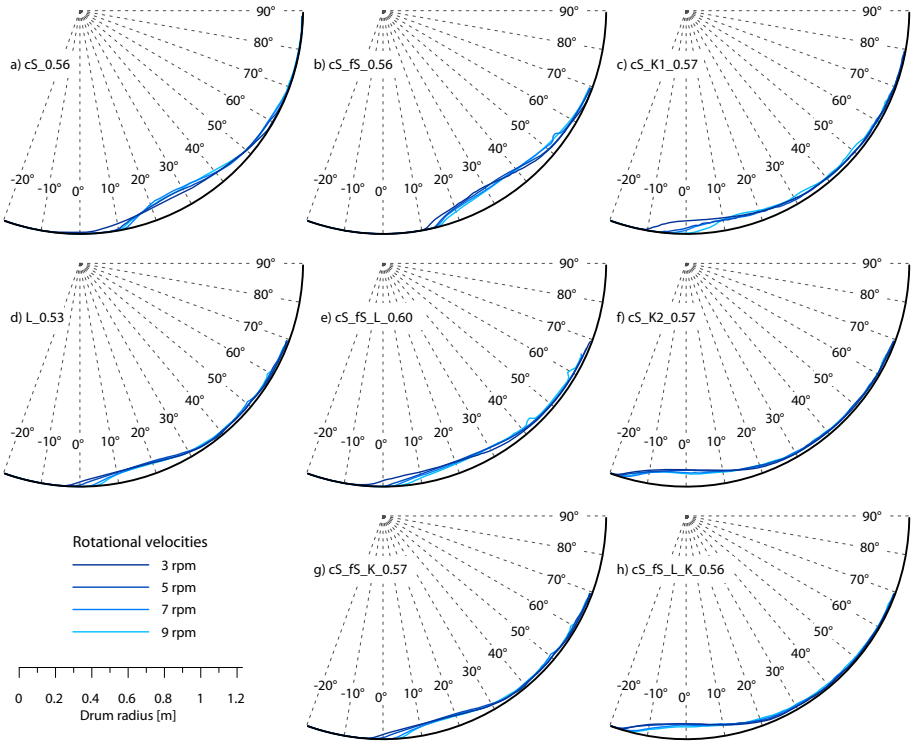

Fig. 6. Mixtures height profiles at different rotational velocities. a) cS_0.69, b) cS_fS_0.69, c) cS_K1_0.68, d) L_0.68, e) cS_fS_L_0.69, f) cS_K2_0.69, g) cS_fS_K_0.68, h) cS_fS_L_K_0.67.

Localization of the front of the flow typically shifts to higher inclinations with the increase of the rotational velocity of the drum, and could be understood as the mixture's response to a change in shear stress resulting in a re-placement of the flow geometry.

Note that for the cS_0.56 test at a rotational velocity of 3 rpm a flat front is developed. Then, as the velocity of the drum is increased, the flow moves up and a bump front is observed. The flat front regards to the percolated water mentioned before and is not obtained in the cS_fS_0.56 test. This is attributed to the reduced porosity of the system, being small enough to keep the volume of water mixed in the soil mixture. For the L_0.53 test, the front of the mixture is located between $-5°$ to $5°$.

When the mixture of sand (cS_fS) is tested with the loess the location of the front remains more likely to the L_0.53 test than to the cS_fS_0.56 test, showing that the behaviour of the loess mixture prevails over the sand mixture. In the case of kaolin the two previous behaviours are observed. First, keeping the same amount of kaolin in the mixture and varying the porosity of the sand media (tests cS_K1_0.57 and cS_fS_K_0.57) a compact flowing mass is obtained as an effect of a decreased porosity. Second, the viscous behaviour of kaolin (cS_K1_0.57 and cS_K2_0.57) is observed to be dominant than the sand interactions, even in the case of a wide PSD (cS_fS_L_K_0.56).

Fig. 7 presents the transition of the location of the front for the cS and L test with the addition of water at different rotational velocities. In the dry case of the cS test the location of the front is not strongly affected by the rotational velocity of the drum (variation of 2°). When water is added to the cS mixture, at a Cv value of 0.65, a re-localization of the front moving up inside the drum is observed. Then, at higher water contents (lower Cv values) the front of the mixture moves downward, and match with the loess tests transition surface. The initial re-localization of the front is attributed to the stronger effect of water in the soil mixture, showing a transition where the partial saturation of the mixture strengths the flow and then dissipates when it reaches and exceeds saturation.

The thin tails observed for flows with an increased viscosity give a probable scenario for mass losses at high solid concentrations (Fig. 6), implying that for the cases where the thickness of the tail is not able to counteract the applied shear stress a fraction of it is dragged upstream.

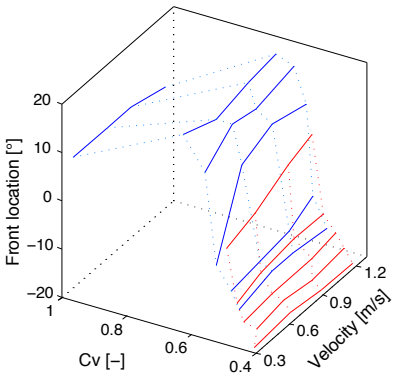

Fig. 7. Localization of the front of the flow for the coarse sand (cS) and loess (L) varying the Cv of the mixture and the rotational velocity of the drum

Considering a constant bulk water content it is possible to infer the following scenarios: a) With the addition of fines mixed with water the density of the fluid rises, the bouyancy of the system increases, and the grain's frictional interactions decreases; and b) As the fines-water mixtures surround the grains, the shear-dependent behaviour induced by the grain-fluid interactions controls the behaviour of the mixture, damping the grain's collisions. Even when it is not possible to differ which of the two scenarios prevails, it is clear that the addition of fines-water mixtures to a granular mass will effect the frictional and collisional interactions of the grains.

As outlined in section 1 the flow behaviour of different mixtures may be connected to the relation of the mean shear stress (τ_{mean}) against the induced shear rate ($\dot{\gamma}$) acting on the flow. Three common behaviours are observed, 1) a shear independent behaviour for the dry coarse sand test (cS_dry) where the variation of the rotational velocity do not vary the shear stress in the mixture. 2) a shear dependent behaviour in which an increase in the rotational velocity increases the shear stresses in the flow, and 3) a shear behaviour in which an increase in the rotational velocity does not increase the shear stress in the flow. Fig. 8 presents the summary of the tests where a shear dependant behaviour was obtained (filled dots and lines).

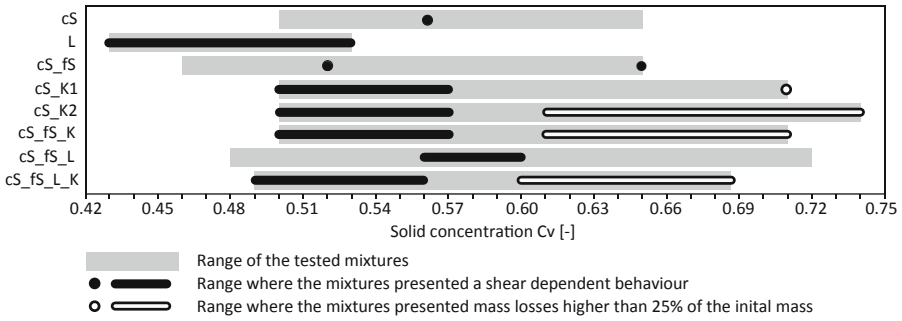

Fig. 8. Experimental range of solid concentrations Cv over the tested mixtures

On the case of the granular mixtures without the addition of an increased viscous fluid (tests cS and cS_fS) it was unexpected to find a shear dependent behaviour (Fig. 8). This is because, it was theorized that sand-flows under low shear stresses were purely frictional, and due to the low viscosity of water (ν of the order of 10^{-3} Pas) the interactions of the grains will prevail over the fluid phase.

On the mixtures with the addition of an increased viscous fluid (tests with kaolin and loess), a shear dependent behaviour is observed at Cv values lower than 0.57 and 0.60 for the kaolin and loess tests (Fig. 8), which shows the apparent threshold in terms of the Cv for non-Newtonian fluids represented by yield pseudo-plastic model.

For the tests cS_K1, cS_K2, cS_fS_K, and cS_fS_L_K the results are somewhat dependent on the strong material losses at low Cv values (Fig. 8), however with the addition of water the system reaches equilibrium, the material losses dissipates, a considerable fraction of material moves back into the drum's channel, and the obtained shear-dependent behaviour is considered reliable.

5 Conclusions

The present study aimed to characterize the interactions of a mixture of coarse and fine sand with the addition of kaolin and loess. The mixtures were tested in a rotating drum by varying the rotational velocity and solid concentration of the mixtures (Cv and Cv_{fluid}). The experiments provide new laboratory evidence of granular mixture behaviour with an increased viscous fluid phase and its characterization. The results show an apparent threshold in terms of Cv where the mixtures started to behave as a shear-dependent material.

The obtained results points that granular flows at high Cv values are controlled by the frictional and collisional interactions. With the addition of water and considering the density and viscosity of the fluid, the grain's interactions are weakened and the stress-strain response of the system is modified. Therefore as the PSD during each test is constant, the classification of the mixture's components as fluid or solid phase is dependent on the stress state inside the flow and not only on a particular particle size threshold.

From the tests developed, the viscous effects of fines-water mixtures on sand granular flows are considered to occur as a result on an increase on the fluid's density which will increase the buoyancy effects on the mixture, and/or the shear-dependent viscous effects originated from the grains-fluid interactions.

Mass losses are a significant limitation, in some cases higher than 25% of the initial mass at high Cv values, and phase separation is significant at low Cv values (presenting a liquid front and a dry tail). These two limits should be considered in future research. While the presented laboratory experiments help to define the experimental field for sand mixtures in the presence of a scaled viscous fluid, the accurate identification of the dominant interactions was not assessed as isolated interactions.

Kaolin and loess were able to induce a non-Newtonian behaviour in the tested mixtures. Their application appears as an interesting alternative to glycerine or other synthetic fluids, in order to represent the solid-fluid interactions in granular flows.

Future studies may focus on the interaction of a scaled viscous fluid with larger granular material components, and on the characteristics of partially saturated flows. Future research may aim to ensure a complete mixture state, in which all the constituents are mixed equally. Furthermore, with the experimental evidence obtained the mechanisms involved in the mass losses are an interesting opportunity to be validated with numerical analysis.

Acknowledgements. The research leading to these results has received funding from the People Programme (Marie Curie Actions) of the European Union's Seventh Framework Programme FP7/2007-2013/ under REA grant agreement n° 289911.

References

1. Barbatoa, C.N., Nelea, M., Pintob, J.C., Franac, S.C.A.: Studies of kaolin rheology. In: IX Jornadas Argentinas de Tratamiento de Minerales, San Juan, Argentina (2008)
2. Brown, S.: The Vertically Rotating Flume for Use as a Rheometer. PhD thesis, University of Missouri-Rolla, USA (1992)
3. Laigle, D., Coussot, P.: Numerical modeling of mudflows. J. Hydraul. Eng. 123, 617–623 (1997)
4. Coussot, P., Meunier, M.: Complex viscosity of a kaolin clay. Clays and Clay Minerals 17, 101–110 (1996)
5. Einstein, H.A.: The bed-load function at high sediment rates. U.S. Dept. of Agriculture, Tech. Bull. 1026 (1950)
6. Franklin, A.G., Krizek, R.J.: Recognition, classification and mechanical description of debris flows. Earth-Science Reviews 40, 209–227 (1996)
7. Gollin, D.: Rheological characterization of debris-flows mixtures using a rotating drum. Master's thesis, Department TESAF Land, Environment, Agriculture and Forestry, University of Padova, Viale dell'Università 16, 35020 Legnaro, PD, Italy (2013)
8. Huizinga, R.: An Analysis of the Two-Dimensional Flow in a Vertically Rotating Flume. PhD thesis, University of Missouri-Rolla, USA (1993)
9. Hungr, O., Evans, S., Bovis, M., Hutchinson, J.: Review of the classification of landslides of the flow type. Environmental and Engineering Geoscience 7, 221–238 (2001)
10. Hungr, O., McDougall, S.: Two numerical models for landslide dynamic analysis. Computers & Geosciences 35(5), 978–992 (2009)
11. Iverson, R.: The physics of debris flows. Reviews of Geophysics 35(3), 245–296 (1997)
12. Iverson, R.M., Denlinger, R.P.: Flow of variably fluidized granular masses across three-dimensional terrain: 1. coulomb mixture theory. Journal of Geophysical Research: Solid Earth 106(B1), 537–552 (2001)
13. Jefferson, I.F., Mavlyanova, N., OHara-Dhand, K., Smalley, I.J.: The engineering geology of loess ground: 15 tasks for investigators - the mavlyanov programme of loes research. Engineering Geology 74, 33–37 (2004)
14. Jop, P., Forterre, Y., Pouliquen, O.: Crucial role of side walls for granular surface flows: consequences for the rheology. J. Fluid Mech. 541, 167–192 (2005)
15. Kaitna, R.: Debris flow experiments in a rotating drum. PhD thesis, University of Natural Resources and Life Sciences, Vienna, Department of Civil Engineering and Natural Hazards, Institute of Mountain Risk Engineering (2006)
16. Kaitna, R., Rickenmann, D., Schneiderbauer, S.: Comparative rheologic investigations in a vertically rotating flume and a moving-bed conveyor belt flume. In: Monitoring, Simulation, Prevention and Remediation of Dense and Debris Flows, pp. 89–98. WIT Press (2006)

17. Kaitna, R., Rickenmann, D.: A new experimental facility for laboratory debris flow investigation. Journal of Hydraulic Research 45(6), 797–810 (2007)
18. Kaitna, R., Rickenmann, D., Schatzmann, M.: Experimental study on rheologic behaviour of debris flow material. Acta Geotechnica 2(2), 71–85 (2007)
19. Kaitna, R., Hsu, L., Rickenmann, D., Dietrich, W.E.: On the development of an unsaturated front of debris flows. In: Genevois, R., Hamilton, D.L., Prestininzi, A. (eds.) 5th International Conference on Debris-Flow Hazards: Mitigation, Mechanics, Prediction and Assessment, Padua, June 14-17, pp. 351–358 (2011), Italian Journal of Engineering Geology and Environment
20. Kaitna, R., Dietrich, W.E., Hsu, L.: Surface slopws, velocity profiles and fluid pressure in shallow, coarse granular flows saturated with water and mud. Manuscript submitted for publication (2013)
21. Parson, J.D., Whipple, K.X., Simon, A.: Experimental study of the grain-flow, fluid-mud transition in debris flows. The Journal of Geology 109, 427–447 (2001)
22. O'Brien, J., Julien, P.: Laboratory Analysis of Mudflow Properties. Journal of Hydraulic Engineering 114(8), 877–887 (1988)
23. Pudasaini, S., Hutter, K.: Avalanche Dynamics: Dynamics of Rapid Flows of Dense Granular Avalanches. Springer, New York (2007)
24. Pudasaini, S.P.: A general two-phase debris flow model. Journal of Geophysical Research: Earth Surface 117(F3), 1–28 (2012)
25. Savage, S., Hutter, K.: The motion of a finite mass of granular material down a rough incline. J. Fluid Mech. 199, 177–215 (1989)
26. Schneider, D., Kaitna, R., Dietrich, W., Hsu, L., Huggel, C., McArdell, B.: Frictional behavior of granular gravelice mixtures in vertically rotating drum experiments and implications for rockice avalanches. Cold Regions Science and Technology 69(1), 70–90 (2011)
27. Smalley, I.J., Jefferson, I.J., OHara-Dhand, K., Evens, R.D.: An approach to the problem of loess deposit formation: Some comments on the in situ or soil-eluvial hypothesis. Quaternary International 152-153, 109–117 (2006)
28. Takahashi, T.: Debris flow: mechanics, prediction and countermeasures. Taylor & Francis, Leiden (2007)